HHS Public Access

Author manuscript

J Dent Res. Author manuscript; available in PMC 2016 July 19.

Published in final edited form as:

J Dent Res. 2001 July ; 80(7): 1621–1624.

Tuned Aperture Computed Tomography to Evaluate Osseous Healing

M.K. Nair[1,*], **A. Seyedain**[1], **S. Agarwall**[1], **R.L. Webber**[2], **U.P. Nair**[1], **N.P. Piesco**[1], **M.P. Mooney**[1], and **H.-G. Grondahl**[3]

[1]Oral and Maxillofacial Radiology, Periodontics, Oral Biology, University of Pittsburgh, G-l 19 Salk Hall, 3501 Terrace Street, Pittsburgh, PA 15261-1923, USA

[2]School of Medicine, Wake Forest University, Winston-Salem, NC, USA

[3]Oral and Maxillofacial Radiology, Göteborg University, Sweden

Abstract

Quantification of osseous healing is a challenging task, requiring expensive advanced imaging modalities. To improve diagnostic osseous imaging, we undertook this prospective study to explore the potential of Tuned Aperture Computed Tomography®. Eighty defects in 20 rabbit mandibles, randomly carrying an osteoblast suspension or a polymer matrix or a combination thereof or no treatment, were imaged at 3, 6, 9, and 12 weeks post-surgery. TACT slices, iteratively restored TACT, and conventional digital radiographs were evaluated. Mean-gray-value distribution within regions of interest was correlated with histomorphometric data. Lesions treated with osteoblast/polymer-matrix delivery systems demonstrated the highest mean gray-value, while the diagnostic efficacy of TACT-IR was significantly better than that of other imaging modalities ($p < 0.001$). Thus, TACT is an accurate imaging modality for non-destructive quantification of osseous dynamics.

Keywords

tomography; digital; osseous; computed; mandible

INTRODUCTION

The radiographic monitoring of osseous defect healing by means of conventional imaging techniques is challenging because of the relative difficulties in distinguishing features of variations in projection geometry from clinically relevant changes in the configuration of the region of interest (ROI). In general, resolving this problem requires the acquisition of three-dimensional (3D) information (Webber *et al.*, 1997). There are several promising advanced imaging modalities currently available that could be adapted for this purpose, such as computed tomography and magnetic resonance imaging. Moreover, quantitative computed tomography (QCT) was designed specifically with such applications in mind. However, their complexity, relative cost, the need for the subject to be immobilized for long periods, and the

*corresponding author, mkn2@pitt.edu.

need for the establishment of practical means for spatial registration of ROIs in 3D between successive examinations have precluded their practical application in laboratory (*in vivo*) and clinical settings.

This study was designed to evaluate Tuned-aperture Computed Tomography (TACT®) for the detection of healing differences in rabbit mandibles. TACT is a 3D image-forming algorithm that could be implemented with virtually any projection-based imaging system capable of digitized output. It produces true 3D data from any number of arbitrarily oriented two-dimensional (2D) projections (Webber *et al.*, 1996, 1997; Nair *et al.*, 1998; Yamamoto *et al.*, 1998; Webber and Messura, 1999). It differs from existing modalities in that it computes the 3D representation using information acquired from known fiducial relationships in 2D projections. This is in contrast to the conventional method, wherein reconstruction is accomplished from "back projections" relative to a fixed-projection geometry designed into the associated hardware. The rigid geometric constraint imposes a practical consequence in that high-quality 3D reconstruction requires nearly complete immobilization of the ROI throughout the entire period of data acquisition. Since TACT produces precise 3D reconstructions from multiple 2D projections whose geometries need not be known in advance, respective projections characterized by inadvertent movement of a rigid ROI between exposures yield no appreciable 3D image degradation. Its numerous advantages lead us to consider its adaptation for the quantitative assay of osseous dynamics in a controlled laboratory environment.

The null hypotheses for this study were that no statistically significant correlation exists between the mean-gray-level distributions within an ROI encompassing the defect (1) and osseous integration, as determined histologically, based on imaging modality; AND with respect to: (2) treatment modalities, (3) time elapsed post-surgery, and (3) site (anterior vs. posterior) or side (left *vs.* right side) of the mandible, as evaluated from displays with all imaging modalities.

MATERIALS & METHODS

Induction of Osteogenesis in Mandibular Bone Defects in Rabbits

The study protocol was approved by the Institutional Animal Care and Use Committee of the University. Twenty New Zealand rabbits were used in this study. One of the investigators, using a slow-speed straight fissure bur, induced 2 two-walled defects 8 mm wide and from 8 to 10 mm apart in each quadrant along the inferior margin (N = 80). Groups of 5 animals randomly received one of the following treatments in each defect: (a) none (control), (b) poly-lactide/polyglycolide (50:50) film–polymer matrix [PM] alone, (c) poly-lactide/polyglycolide (50:50) film impregnated with autologous osteoblasts [OS-PM], and (d) osteoblasts in suspension grown *in vitro* [OS] (Table 1). These groups of rabbits were killed following a post-surgical healing period of 3, 6, 9, or 12 wks, and the mandibles were subjected to histo-morphometric evaluation.

Direct digital images were produced by use of the tube-head of a programmable imaging unit (OP-100, Instrumentarium Imaging, Milwaukee, WI, USA), customized for TACT imaging (OrthoTACT®). Projections were captured by use of the Schick #2-size sensor

(Schick Technologies, Long Island City, NY, USA), which was mounted lingual to the mandible, by means of a positioner (Rinn Corporation, Elgin, IL, USA). A fiduciary marker, 1.5 mm in diameter, was attached approximately 3 mm buccal to the ROI to facilitate image reconstruction. We positioned the x-ray source for each exposure along a curved locus of the movable tube head, using arbitrary projection geometry of 9° to 20° to either side of the central projection axis (Nair *et al.*, 1998), resulting in 9 projections. The exposure parameters used were 65 kVp, 15 mA, and 0.1 sec, with a source-to-object distance of 40 cm. Thus, 3 imaging modalities were available for evaluation purposes: (a) two-dimensional digital images, (b) TACT slices (TACT-S), and (c) iteratively restored TACT (TACT-IR), with tomosynthetic artifacts subtracted (Nair *et al.*, 1998; Liang *et al.*, 1999).

Slices through comparable planes were evaluated across all specimens. Analysis of the gray-level distribution involved histogram equalization with respect to a reference image, and selection of an ROI within each site by an observer. This was then referenced so that it could be applied to homologous sites across all specimens. Three observers, blinded as to the variables involved and the results of histomorphometry, read the images. The gray-value distribution (**AQ**) and standard deviation within each ROI were computed by means of the TACT workbench. Five measurements were made within each site by each observer in two sittings, separated by 2 wks. The scores were then averaged for each ROI (Table 2).

The animals were killed by an overdose of Nembutal. The mandibular blocks were fixed in 10% neutral buffered formalin, and decalcified in 10% formic acid. The tissues were embedded in paraffin and sectioned sagitally and axially. Resulting 6- to 8-mm-thick sections were stained with hematoxylin and eosin and examined microscopically. The sections were scored on a scale of 0 to 10, where 0 represented no bone formation and 10, complete osseous healing of the defect.

Correlation between the mean-gray-value distribution and histologic data was computed by Pearson's correlation coefficient. Alpha was pre-set at 0.05.

RESULTS

ANOVA revealed a statistically significant difference in the mean gray-values based on treatment modality ($p < 0.001$), imaging modality ($p < 0.001$), time after surgery ($p < 0.039$), site ($p < 0.004$), and side ($p < 0.022$). The mean-gray-value distribution was the highest for OS-PM, followed by PM alone, OS alone, and control sites, respectively (Table 2) at $p < 0.001$. Higher mean gray-values were also noted for (1) iteratively restored TACT, (2) posterior lesions, (3) lesions on the right side, and (4) post-surgical healing periods of 9 or more wks (Table 2). These differences were significant for the following groups time-wise: 3 and 9 wks ($p < 0.001$), 6 and 9 wks ($p < 0.001$), 3 and 12 weeks ($p < 0.001$), and 6 and 12 wks ($p < 0.01$). Based on imaging modalities, TACT-IR differed from all other imaging modalities at $p < 0.001$. With respect to the sides and sites of lesions, it was noted in Tukey's analyses that the right sides of the mandibles demonstrated a higher mean gray-value ($p < 0.04$), as did the posterior sites ($p < 0.003$), at all times and across all imaging modalities.

Pair-wise comparisons of mean-gray-value distributions revealed that TACT-IR recorded the highest mean-gray-value distribution across all treatment modalities, followed by TACT-S and Dl, with sites carrying OS-PM recording the highest value (Table 3). Based on tine post-surgery, the mean-gray-value distribution continued to be the highest with TACT-IR images among all imaging modalities, with little change, or sometimes a lower mean gray-value being recorded at week 12 as compared with week 9. Interactions between treatment modality and time revealed that the highest mean gray-value was recorded for OS-PM at all times.

Fig. a illustrates the comparison among radiographic examinations instituted for this study, where a distinct ossific bridge across the defect in a site treated with OS-PM is revealed clearly in the TACT-IR image. Fig. b illustrates the histological analysis of the defect, showing bone formation above the inferior alveolar nerve, paralleling the results of image analysis performed by TACT.

Pearson's correlation coefficient for each imaging modality revealed the highest correlation between mean-gray-value distribution (radiometric data) and new bone formation (histologic data) for TACT -IR, followed by TACT-S and conventional radiographs (0.84, 0.77, and 0.52, respectively). Interclass correlation coefficient computed to evaluate inter-observer agreement was 0.79, indicating good inter-observer reliability.

DISCUSSION

An experimental design involving surgical induction of representative defects was selected over a passive model based on identification of naturally occurring lesions, because the latter are relatively rare and their morphology varies significantly with etiology. Previous studies showed that two-walled defects in rabbit mandibles, 5 mm or larger, did not heal over 52 wks post-surgery (Schmitz and Hollinger, 1986; Hollinger and Klineschmidt, 1990). However, our pilot studies using a polymer matrix (Atrix Laboratories, Fort Collins, CO, USA) indicated resolution of defects as large as 8 mm in 12 wks. Therefore, we elected to evaluate healing over 3–12 wks.

The fact that known healing variations confirmed histomorphologically were correlated significantly with observations derived non-destructively from *in vivo* specimens demonstrates the potential of TACT for the evaluation of osseous healing with conventional radiographic projections as source data. The mean-gray-value distribution computed from TACT-IR provided the most correlation with the histomorphometric data, followed by TACT-S and conventional radiographs. Conventional film-based radiographs can also be used to acquire the basis images, although in this study we used direct digital radiographs due to the availability of a digital imaging system entailing lower radiation exposures, without compromising the signal-to-noise ratio.

The highest mean gray-value recorded consistently with OS-PM reveals that healing was favored in instances where osteoblasts were available in the presence of adequate scaffolding material. It seems apparent that detectable healing effects are determined equally by the experimental conditions underlying lesion management and the period over which healing is

evaluated under the experimental conditions imposed by the investigation. The significance of time after surgery on the rate of healing was anticipated in the light of pilot studies where the same experimental design was used. This observation is not the result of unknown sources of statistical variation or system non-linearities that usually preclude detection of subtle changes with time, since histomorphometric analyses reveal osseous tissue formation very early in the healing process. The significant differences noted in the healing process time-wise may be due to possible maturation of bone that has already formed.

These results provide speculative bases for economically attractive alternatives to QCT and other existing high-tech methods for the evaluation of osseous changes in 3D (Fuhrmann *et al.*, 1995; Langen *et al.*, 1995; Matteson *et al.*, 1996; Dado *et al.*, 1997; Rosenstein *et al.*, 1997). TACT capitalizes on the fact that projection differences between individual homologous slices in a 3D ROI are less influenced by modest variations in projection geometry between examinations than by differences produced from 2D projections of the same region. Hence, this study compared data from TACT-generated density measurements of the ROIs with data produced from 2D projections, with information from histomorphometry as ground truth.

In conclusion, TACT has been shown to be an accurate method for facilitation of non-destructive assessment of osseous healing in rabbit mandibles, and by virtue of its flexibility and relative simplicity, warrants consideration as a cost-effective alternative or supplement to existing 3D-imaging modalities for a variety of clinical applications.

Acknowledgments

This study was supported in part by the Pittsburgh Tissue Engineering Institute; SBIR Awards/NIH; CMRF, University of Pittsburgh; Atrix Laboratories, Colorado; and Instrumentarium Imaging, Finland. The study received the Charles Morris Award from the American Academy of Oral and Maxillofacial Radiology.

REFERENCES

Dado DV, Rosenstein SW, Alder ME, Kernahan DA. Long-term assessment of early alveolar bone grafts using three-dimensional computer-assisted tomography: a pilot study. Plast Reconstr Surg. 1997; 99:1840–1845. [PubMed: 9180707]

Fuhrmann RA, Wehrbein H, Langen HJ, Diedrich PR. Assessment of the dentate alveolar process with high resolution computed tomography. Dentomaxillofac Radiol. 1995; 24:50–54. [PubMed: 8593909]

Hollinger JO, Kleinschmidt JC. The critical size defect as an experimental model to test bone repair materials. J Craniofac Surg. 1990; 1:60–68. [PubMed: 1965154]

Langen HJ, Fuhrmann R, Diedrich P, Gunther RW. Diagnosis of infra-alveolar bony lesions in the dentate alveolar process with high-resolution computed tomography. Experimental results. Invest Radiol. 1995; 30:421–426. [PubMed: 7591651]

Liang H, Tyndall DA, Ludlow JB, Lang LA. Cross-sectional presurgical implant imaging using tuned aperture-computed tomography (TACT™). Dentomaxillofac Radiol. 1999; 28:232–237. [PubMed: 10455387]

Matteson SR, Deahl ST, Alder ME, Nummikoski PV. Advanced imaging methods. Crit Rev Oral Biol Med. 1996; 7:346–395. [PubMed: 8986396]

Nair MK, Tyndall DA, Ludlow JB, May K, Ye F. The effects of restorative material and location on the detection of simulated recurrent caries. A comparison of dental film, direct digital radiography and tuned aperture computed tomography. Dentomaxillofac Radiol. 1998; 27:80–84. [PubMed: 9656871]

Rosenstein SW, Long RE Jr, Dado DV, Vinson B, Alder ME. Comparison of 2-D calculations from periapical and occlusal radiographs versus 3-D calculations from CAT scans in determining bone support for cleft-adjacent teeth following early alveolar bone grafts. Cleft Palate Craniofac J. 1997; 34:199–205. [PubMed: 9167069]

Schmitz JP, Hollinger JO. The critical size defect as an experimental model for craniomandibulofacial nonunions. Clin Orthop. 1986; 205:299–308. [PubMed: 3084153]

Webber RL, Messura JK. An in vivo comparison of diagnostic information obtained from tuned-aperture computed tomography and conventional dental radiographic imaging modalities. Oral Surg Oral Med Oral Pathol Oral Radiol Endod. 1999; 88:239–247. [PubMed: 10468470]

Webber RL, Horton RA, Underhill TE, Ludlow JB, Tyndall DA. Comparison of film, direct digital, and tuned-aperture computed tomography images to identify the location of crestal defects around endosseous titanium implants. Oral Surg Oral Med Oral Pathol Oral Radiol Endod. 1996; 81:480–490. [PubMed: 8705598]

Webber RL, Horton RA, Tyndall DA, Ludlow JB. Tuned-aperture computed tomography (TACT). Theory and application for three-dimensional dento-alveolar imaging. Dentomaxillofac Radiol. 1997; 26:53–62. [PubMed: 9446991]

Yamamoto K, Farman AG, Webber RL, Horton RA, Kuroyanagi K. Effects of projection geometry and number of projections on accuracy of depth discrimination with tuned-aperture computed tomography in dentistry. Oral Surg Oral Med Oral Pathol Oral Radiol Endod. 1998; 86:126–130. [PubMed: 9690258]

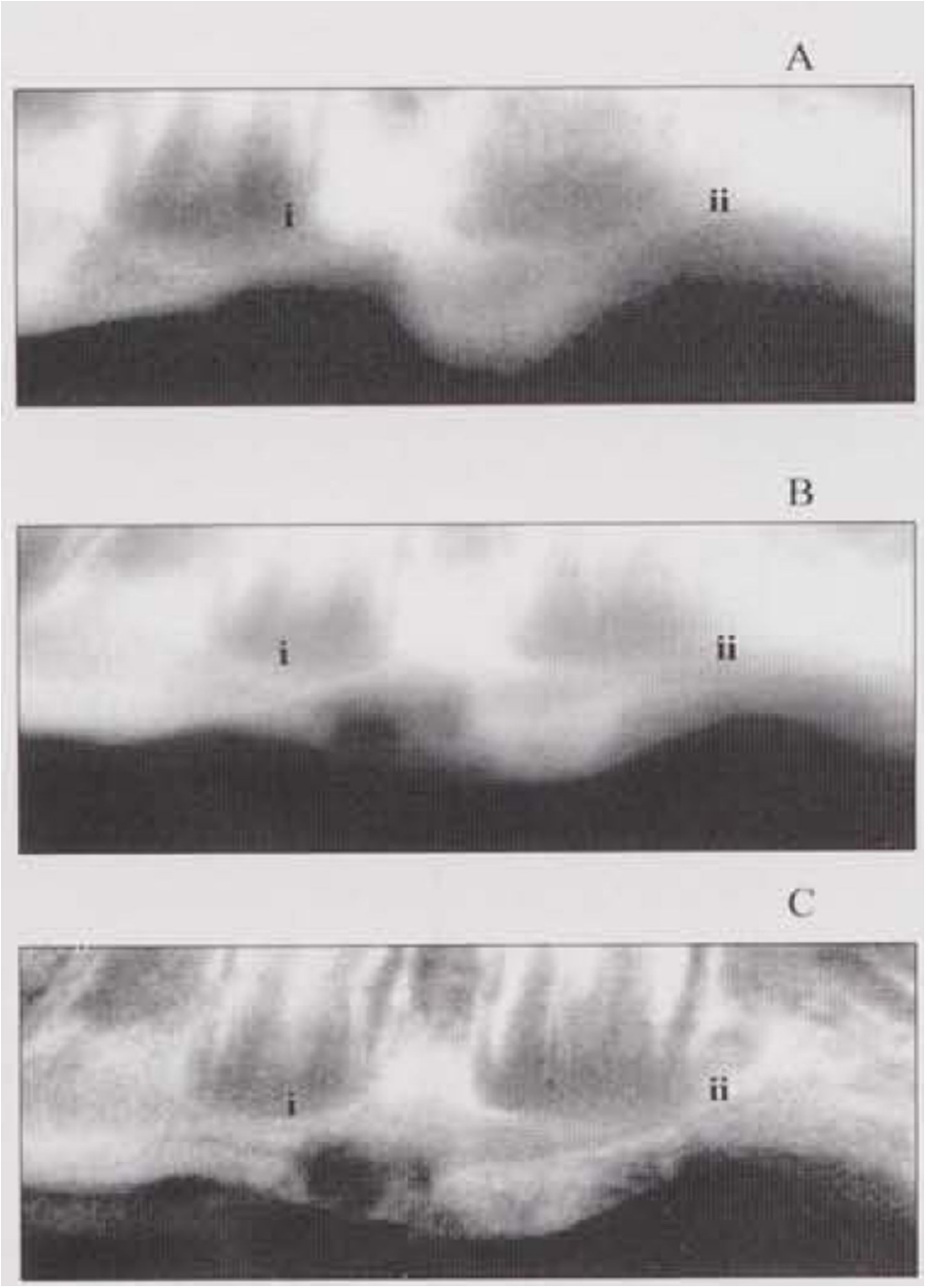

Figure (a).

Representative images of the same specimen: **(A)** direct digital image; **(B)** unprocessed TACT **(C)** iteratively restored TACT. Anterior and posterior lesions depicted were subject to: (i) osteoblast-polymer-matrix graft, and (ii) no treatment. The extent of healing of the defect (i) is more evident in **(C)**, where an ossific bridge is visible.

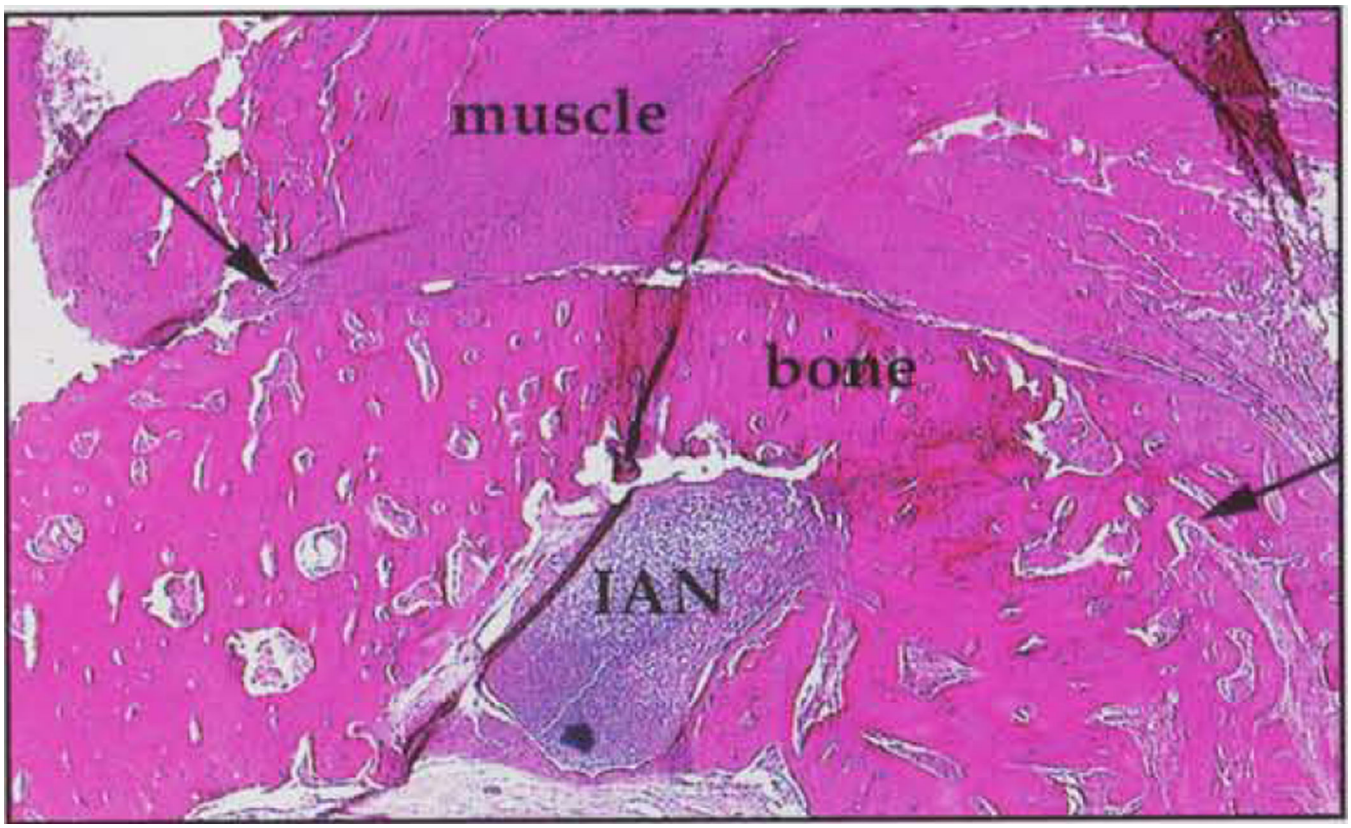

Figure (b).
Histological examination of defect in (a). Defect (arrows) shows bone formation where osteoblast/polymer-matrix system was allowed to heal for 8 wks. IAN = inferior alveolar nerve.

Table 1

Experimental Design

Specimen	Quadrant	Site	Treatment	Death (wks)
1 – 5	Left	Anterior		
		Posterior		
	Right	Anterior		3
		Posterior		
		Anterior		
	Left	Posterior	Polymer-matrix; OR	
6 – 10		Anterior	Polymer-matrix with osteoblasts; OR	6
	Right	Posterior		
		Anterior	Osteoblasts; OR	
	Left	Posterior	No treatment.	
11 – 15		Anterior		9
	Right	Posterior		
		Anterior		
	Left	Posterior		
16 – 20		Anterior		12
	Right	Posterior		

Table 2

Note Increases in Mean-gray-value Distributions (in bold) for: (1) Sites Carrying Osteoblast-Polymer Combination; (2) Iteratively Restored TACT, (3) Posterior Lesions, (4) 9 or More Wks Post-surgery, and (5) Lesions on the Right Side

Effect	Type	Mean Gray-value (SD)
Treatment	Controls	62 (13.7)
	Polymer-matrix only	66 (13.4)
	Osteoblasts only	64 (12.2)
	Osteoblast/polymer-matrix	**76 (13.2)**
Image	TACT slices	62 (9.9)
	Iteratively restored TACT	**78 (9.1)**
	Two-dimensional digital	61 (9.3)
Location	Anterior	65 (9.9)
	Posterior	**69 (9.4)**
Time (wks)	Three	60 (9.2)
	Six	64 (9.6)
	Nine	**70 (9.2)**
	Twelve	**70 (9.5)**
Side	Right	**67 (9.9)**
	Left	66 (9.6)

Table 3

Matrices of Pair-wise Comparisons of Mean-gray-value Distribution Based on Interactions among Imaging, Treatment Modality, and Time after Surgery

Imaging *vs.* Treatment Modality				
	Controls	**Polymer-matrix**	**Osteoblasts**	**Polymer-matrix-osteoblasts**
Digital images	55.4 (11.2)[a]	60.0 (12.7)[a]	56.7 (10.8)[a]	73.3 (14.9)[a]
Iteratively restored TACT	73.4 (9.3)[a]	75.5 (8.7)[a]	74.0 (8.9)[a]	85.5 (12.7)[a]
TACT slices	57.8 (10.4)[a]	62.0 (8.9)[a]	61.2 (9.6)[a]	68.6 (8.2)[a]
Time *vs.* Treatment Modality				
	3wks	6wks	9wks	12wks
Digital images	58.5 (11.7)[a]	57.3 (12.4)[a]	64.1 (12.4)[a]	65.1 (15.0)[a]
Iteratively restored TACT	68.2 (10.2)[a]	73.9 (10.6)[a]	83.6 (12.4)[a]	80.9 (15.2)[a]
TACT slices	56.1 (7.3)[a]	62.0 (9.0)[a]	64.4 (11.3)[a]	65.3 (9.5)[a]
Time *vs.* Treatment Modality				
	3wks	6wks	9wks	12wks
No treatment	59.4 (10.0)[a]	61.4 (12.9)[a]	62.4 (16.3)[a]	65.6 (14.7)[a]
Polymer-matrix	60.6 (12.8)[a]	64.2 (10.4)[a]	67.1 (16.3)[a]	71.7 (12.4)[a]
Osteoblasts only	57.2 (10.3)[a]	61.6 (13.9)[a]	66.2 (10.7)[a]	69.0 (12.3)[a]
Polymer-matrix/osteoblast	67.5 (8.9)[a]	70.2 (13.3)[a]	81.5 (10.9)[a]	82.5 (15.8)[a]

[a]Standard deviation.